LETTER

Novel 2,4-Diarylaminopyrimidine Derivatives Containing Pyridine Moiety: Design, Synthesis, Crystal Structure and Biological Evaluation①

LIU Ju[a, b, c] WU Shuang[a] WANG Huan[a] DU Si-Yuan[a]
LI Zhen[a] SHEN Ji-Wei[a, b, c] CHEN Ye[a, b, c②] DING Shi[a, b, c②]

[a] (*College of Pharmacy of Liaoning University, Shenyang* 110036, *China*)

[b] (*API Engineering Technology Research Center of Liaoning Province, Shenyang* 110036, *China*)

[c] (*Small Molecular Targeted Drug R&D Engineering Research Center of Liaoning Province, Shenyang* 110036, *China*)

ABSTRACT A series of 2,4-diarylaminopyrimidine derivatives containing pyridine structure were designed and synthesized. The crystal structures of compounds **5d** and **5e** were obtained from X-ray diffraction. The crystal structure of **5d** ($C_{25}H_{20}ClFN_6O_2$) belongs to the monoclinic system, space group $P2_1/c$ with a = 11.0500(10), b = 18.3045(17), c = 13.5646(9) Å and β = 122.806(5)°. **5e** ($C_{25}H_{19}ClF_2N_6O_2$) is of monoclinic system, space group $P2_1/c$ with a = 10.9998(18), b = 18.517(3), c = 13.6355(16) Å and β = 123.315(9)°. The bioassay results showed all of the target compounds exhibited potential antiproliferative activities against MKN-45, HT-29, A549, K562 and GIST882 cell lines. Among them, compounds **5a**, **5c** and **5e** exhibited remarkable inhibitory activities against GIST882, K562 and A549 cell lines with IC_{50} values of 0.68, 0.38 and 0.60 μM, respectively, which were comparable to that of the positive control foretinib.

Keywords: **pyrimidine, pyridine, synthesis, X-ray diffraction, antitumor activity;**

DOI: 10.14102/j.cnki.0254-5861.2011-3283

1 INTRODUCTION

Cancer is one of the most health problems in the world. Although many classes of drugs were used for the treatment, the needs for safe and effective anticancer compounds are still significant target[1, 2]. Pyridine and pyrimidine-based compounds have been reported to show remarkable antitumor activities by means of inhibiting multiple enzymes, and some of them are already being marketed or are under clinical/preclinical studies, such as imatinib, sorafenib, crizotinib, abiraterone, BMS-794833, altiratinib, and BMS-777607[3-6]. Among above compounds, BMS-794833, altiratinib, and BMS-777607 are representative 4-phenoxypyridine based type II c-Met kinase inhibitors[7, 8]. Blocking c-Met kinase activity by small-molecule inhibitors has been identified as a promising approach for the treatment of cancers[9].

As described in Fig. 1, structurally, most of 4-phenoxypyridine type II c-Met inhibitors may be disconnected into three moieties: a 4-phenoxypyridine core (moiety A), a phenyl or substituted phenyl group (moiety B) and a linker bridge (moiety C). Moiety A and moiety B are crucial for kinase activity[10-12]. With the goal of finding more 4-phenoxypyridine-based antitumor agents, *N*-[4-(2-fluorophenoxy)pyridin-2-yl]cyclopropanecarboxamide was used as the moiety A. Pyrimidine-2,4-diamine was introduced into the moiety C *via* cyclization strategy. Furthermore, various substituents were introduced at the phenyl ring (moiety B) to investigate their effects on activities (Fig. 1). Accordingly, a series of 4-phenoxypyridine derivatives were designed, synthesized and evaluated for their *in vitro* antiproliferative activities

Received 10 June 2021; accepted 10 August 2021 (**CCDC 2088950 for 5d and 2088951 for 5e**)

① Supported by the Youth National Natural Science Foundation of China (21807055), the General Project of Education Department of Liaoning Province (LJC201907), Natural Science Foundation of Liaoning Provincial Department of Science and Technology (2019-ZD-0191), and the College Students' Innovation and Entrepreneurship Training Program of Liaoning University (D202011280014195636)

② Corresponding authors. Ding Shi (1986-), PhD and associate professor, majoring in medical chemistry. E-mail: dingshi_destiny@163.com; Chen Ye (1965-), professor, majoring in medical chemistry. E-mail: sy-chenye@163.com

against MKN-45, HT-29, A549, K562 and GIST882 cancer cell lines.

2 EXPERIMENTAL

2. 1 Materials and methods

Unless otherwise specified, all materials were obtained from commercial suppliers and were used without further purification. ^{1}H NMR spectra were recorded on a Bruker Biospin 600 MHz instrument using TMS as the internal standard. All chemical shifts were reported in ppm. IR spectra were recorded as KBr pellets on a Perkin-Elmer Spectrum one FT-IR spectrometer. MS spectra were obtained on an Agilent 6460 QQQ mass spectrometer (Agilent, USA) analysis system. Crystal data were obtained on a Bruker P4 X-diffractometer.

2. 2 Synthesis of *N*-(4-chloropyridin2-yl)-cyclopropylformamide (1)

Cyclopropanecarbonyl chloride (9.30 g, 89.00 mmol) was dissolved in dried CH_2Cl_2 (30 mL) and dropwise added to a mixture of 4-chloropyridin-2-amine (8.80 g, 68.45 mmol), Et_3N (20.78 g, 205.35 mmol) and CH_2Cl_2 (80 mL) in an ice bath, which was then removed to raise the temperature to room temperature and stirred for 12 h. The resulting mixture was sequentially washed with 20% K_2CO_3 (50 mL × 3) and brine (50 mL × 3), and the organic phase was separated, dried over anhydrous Na_2SO_4, filtered, and the filtrate was evaporated under reduced pressure. The crude product obtained was purified by silica gel chromatography to give 9.78 g (yield: 73%) of **1** as a white solid. IR (KBr) cm^{-1}: 3242(-NH-), 1707(C=O), 1670, 1588(C=N), 1574(Ar), 1537(Ar), 1404, 1257, 1213, 1190, 1150, 960, 873, 824, 710; ^{1}H NMR (600 MHz, $CDCl_3$) δ 8.79 (s, 1H), 8.31 (s, 1H), 8.16 (d, J = 5.4 Hz, 1H), 7.03 (dd, J = 5.4, 1.6 Hz, 1H), 1.60~1.49 (m, 1H), 1.17~1.09 (m, 2H), 0.97~0.87 (m, 2H); MS (ESI) m/z (%): 197.1 $[M+H]^+$.

2. 3 Synthesis of *N*-(4-(2-fluoro-4-nitro-phenoxy)pyridin-2-yl)cyclopropylformamide (2)

A stirring mixture of compound **8** (8.00 g, 40.68 mmol) and 2-fluoro-4-nitrophenol (15.98 g, 101.71 mmol) in chlorobenzene (100 mL) was refluxed for about 40 h. After cooling to room temperature, the reaction mixture was concentrated under reduced pressure to yield a pale solid. The solid was dissolved in CH_2Cl_2 (150 mL), washed with saturated K_2CO_3 aqueous solution (80 mL × 4) and then brine (60 mL × 4), dried over anhydrous Na_2SO_4, and finally concentrated under reduced pressure to afford a brown solid, which was purified by silica gel chromatography to give 7.13 g (yield: 55%) of **2** as a light yellow solid. IR (KBr) cm^{-1}: 3418(-NH-), 1687(C=O), 1617(C=N), 1529(Ar), 1493(Ar), 1354, 1300, 1272, 1180, 1070, 875, 798; ^{1}H NMR (600 MHz, DMSO-d_6) δ 11.00 (s, 1H), 8.43 (dd, J = 10.3, 2.2 Hz, 1H), 8.30 (d, J = 5.7 Hz, 1H), 8.19 (dd, J = 9.0, 1.9 Hz, 1H), 7.76 (d, J = 2.2 Hz, 1H), 7.61 (t, J = 8.5 Hz, 1H), 6.86 (dd, J = 5.6, 2.2 Hz, 1H), 2.04~1.95 (m, 1H), 0.78 (t, J = 6.3 Hz, 4H); MS (ESI) m/z (%): 318.1 $[M+H]^+$.

2. 4 Synthesis of *N*-(4-(4-amino-2-fluoro-phenoxy)pyridin-2-yl)cyclopropanecarboxamide (3)

A mixture of compound **2** (6.00 g, 18.91 mmol), iron powder (5.28 g, 94.56 mmol), acetic acid (11.36 g, 189.10 mmol), water (20 mL) and ethyl acetate (100 mL) was heated to reflux for 2 h. After completion of the reaction as indicated by TLC, the mixture was filtered immediately. The organic layer of the filtrate was separated, washed with water, dried over anhydrous Na_2SO_4 and filtered, and the filtrate was evaporated under reduced pressure when white solid appeared, which was filtered to obtain 3.51 g (yield: 65%) of **3** as a white solid. IR (KBr) cm^{-1}: 3411(-NH-), 2026, 1737(C=O), 1618(C=N), 1510(Ar), 1427, 1207, 1163, 993, 956, 866, 822, 610; ^{1}H NMR (600 MHz, DMSO-d_6) δ 10.79 (s, 1H), 8.15 (d, J = 5.7 Hz, 1H), 7.59 (s, 1H), 6.95 (t, J = 9.0 Hz, 1H), 6.67~6.61 (m, 1H), 6.49 (dd, J = 13.1, 2.2 Hz, 1H), 6.40 (d, J = 8.7 Hz, 1H), 5.44 (s, 2H), 2.03~1.88 (m, 1H), 0.76 (br, 4H); MS (ESI) m/z (%): 288.1 $[M+H]^+$, 310.1 $[M+Na]^+$.

2. 5 Synthesis of *N*-(4-(4-((2-chloropyrimidin-4-yl)amino)-2-fluorophenoxy)pyridin-2-yl)cyclopropane formamide (4)

A mixture of compound **3** (3.00 g, 10.44 mmol), 2,4-dichloropyrimidine (1.87 g, 12.53 mmol), and diisopropylethylamine (1.35 g, 10.44 mmol) in isopropanol (50 mL) was heated at reflux for 25 h. Upon cooling to room temperature, the mixture evaporated under reduced pressure. The residue was dissolved in dichloromethane (80 mL), and washed with water (50 mL × 3). The organic layer was dried over anhydrous Na_2SO_4 and concentrated under reduced pressure to afford crude product, which was purified by silica gel chromatography to give 3.17 g (yield: 76%) of **4** as a white solid. ^{1}H NMR (600 MHz, DMSO-d_6) δ 10.90 (s, 1H), 10.34 (s, 1H), 8.25~8.22 (m, 2H), 7.88~7.60 (m, 2H), 7.50~7.30 (m, 2H), 6.85~6.71 (m, 2H), 2.03~1.92 (m, 1H), 0.84~0.72 (m, 4H); MS (ESI) m/z (%): 400.1 $[M+H]^+$, 422.0 $[M+Na]^+$.

2. 6 General procedure for preparing the target compounds (5a~5f)

A mixture of compound **4** (0.20 g, 0.50 mmol), aromatic amine (1.3 equivalents) and *p*-toluenesulfonic acid (1.0 equivalent) in isopropanol (8.0 mL) was refluxed for about 18 h. After cooling to room temperature, the resultant precipitate was filtered and dried under vacuum to afford the target compounds **5a~5f** as white solid.

***N*-(4-(2-fluoro-4-((2-(phenylamino)pyrimidin-4-yl)amino)phenoxy)pyridin-2-yl)cyclopropanecarboxamide (5a)**

Yield: 67%; ^{1}H NMR (600 MHz, DMSO-d_6) δ 10.58 (d, J = 13.1 Hz, 1H), 9.37 (d, J = 11.5 Hz, 1H), 9.05~8.80 (m, 1H), 8.20~8.06 (m, 2H), 8.02 (d, J = 5.7 Hz, 1H), 7.81~7.62 (m, 3H), 7.37 (d, J = 8.4 Hz, 1H), 7.30~7.19 (m, 2H), 7.10 (t, J = 8.8 Hz, 1H), 6.91 (t, J = 7.2 Hz, 1H), 6.65~6.50 (m, 1H), 6.22 (d, J = 5.7 Hz, 1H), 2.04~1.89 (m, 1H), 0.91~0.83 (m, 2H), 0.79~0.72 (m, 2H); MS (ESI) m/z(%): 457.2 $[M+H]^+$, 479.1 $[M+Na]^+$.

***N*-(4-(2-fluoro-4-((2-((4-fluorophenyl)amino)pyrimidin-4-yl)amino)phenoxy)pyridin-2-yl)cyclopropanecarboxamide (5b)**

Yield: 59%; ^{1}H NMR (600 MHz, DMSO-d_6) δ 10.74~10.55 (m, 1H), 9.53~9.32 (m, 1H), 9.16~8.87 (m, 1H), 8.20~7.92 (m, 3H), 7.70 (d, J = 13.4 Hz, 3H), 7.41~7.28 (m, 1H), 7.19~7.04 (m, 1H), 7.04~6.88 (m, 2H), 6.64~6.50 (m, 1H), 6.31~6.12 (m, 1H), 5.86~5.82 (m, 1H), 2.03~1.88 (m, 1H), 0.96~0.58 (m, 4H); IR (KBr, cm^{-1}): 3258(-NH-), 2355, 1678(C=O), 1591, 1508(Ar), 1422(Ar), 1312, 1207, 982, 820; MS (ESI) m/z (%): 475.2 $[M+H]^+$, 497.1 $[M+Na]^+$.

***N*-(4-(4-((2-((4-chlorophenyl)amino)pyrimidin-4-yl)amino)-2-fluorophenoxy)pyridin-2-yl)cyclopropanecarboxamide (5c)**

Yield: 55%; ^{1}H NMR (600 MHz, DMSO-d_6) δ 10.67~10.45 (m, 1H), 9.50~9.31 (m, 1H), 9.18~8.92 (m, 1H), 8.26~7.96 (m, 3H), 7.79~7.67 (m, 3H), 7.35 (d, J = 7.3 Hz, 1H), 7.26~7.00 (m, 3H), 6.59 (dd, J = 5.7, 2.3 Hz, 1H), 6.24 (d, J = 5.7 Hz, 1H), 2.07~1.86 (m, 1H), 0.90~0.83 (m, 2H), 0.79~0.73 (m, 2H); IR (KBr, cm^{-1}): 3281(-NH-), 2353, 1672(C=O), 1585, 1416(Ar), 1308, 1204, 1094, 978, 804, 687; MS (ESI) m/z (%): 491.1 $[M+H]^+$, 513.1 $[M+Na]^+$.

***N*-(4-(4-((2-((3-chlorophenyl)amino)pyrimidin-4-yl)amino)-2-fluorophenoxy)pyridin-2-yl)cyclopropanecarboxamide (5d)**

Yield: 57%; ^{1}H NMR (600 MHz, DMSO-d_6) δ 10.51 (br, 1H), 9.36 (br, 1H), 9.17~9.04 (m, 1H), 8.13 (d, J = 5.7 Hz, 1H), 8.04 (d, J = 5.7 Hz, 1H), 7.95 (s, 1H), 7.92~7.83 (m, 1H), 7.74 (d, J = 1.9 Hz, 1H), 7.57 (d, J = 8.2 Hz, 1H), 7.41 (d, J = 8.8 Hz, 1H), 7.18 (t, J = 8.1 Hz, 1H), 7.12 (t, J = 8.8 Hz, 1H), 6.87 (d, J = 7.9 Hz, 1H), 6.60~6.55 (m, 1H), 6.31~6.22 (m, 1H), 2.03~1.84 (m, 1H), 0.91~0.86 (m, 2H), 0.79~0.74 (m, 2H); IR (KBr, cm^{-1}): 3305(-NH-), 2357, 1679(C=O), 1619, 1416, 1314, 1207, 1105, 990, 808; MS (ESI) m/z (%): 491.1 $[M+H]^+$, 513.1 $[M+Na]^+$.

***N*-(4-(4-((2-((3-chloro-4-fluorophenyl)amino)pyrimidin-4-yl)amino)-2-fluorophenoxy)pyridin-2-yl)cyclopropanecarboxamide (5e)**

Yield: 45%; ^{1}H NMR (600 MHz, DMSO-d_6) δ 10.76~10.50 (m, 1H), 9.48 (d, J = 13.0 Hz, 1H), 9.25 (d, J = 13.9 Hz, 1H), 8.17~8.10 (m, 1H), 8.06~7.97 (m, 3H), 7.71 (d, J = 3.4 Hz, 1H), 7.58 (br, 1H), 7.45~7.33 (m, 1H), 7.20~7.03 (m, 2H), 6.64~6.54 (m, 1H), 6.26 (t, J = 6.8 Hz, 1H), 1.97 (d, J = 4.1 Hz, 1H), 0.92~0.71 (m, 4H); IR (KBr, cm^{-1}): 3269(-NH-), 2349, 1678(C=O), 1591, 1413(Ar), 1310, 1259, 1207, 1101, 990, 808; MS (ESI) m/z (%): 509.1 $[M+H]^+$, 531.1 $[M+Na]^+$.

***N*-(4-(2-fluoro-4-((2-(*p*-tolylamino)pyrimidin-4-yl)amino)phenoxy)pyridin-2-yl)cyclopropanecarboxamide (5f)**

Yield: 62%; ^{1}H NMR (600 MHz, DMSO-d_6) δ 10.63 (s, 1H), 9.38 (s, 1H), 8.85 (s, 1H), 8.16~8.08 (m, 2H), 8.00 (d, J = 0.6 Hz, 1H), 7.72 (s, 1H), 7.57 (d, J = 8.3 Hz, 2H), 7.37 (d, J = 8.7 Hz, 1H), 7.10 (t, J = 8.9 Hz, 1H), 7.07~7.01 (m, 2H), 6.59 (dd, J = 5.7, 2.3 Hz, 1H), 6.19 (d, J = 5.7 Hz, 1H), 2.27 (s, 3H), 2.05~1.90 (m, 1H), 0.89~0.82 (m, 2H), 0.79~0.72 (m, 2H); IR (KBr, cm^{-1}): 3196(-NH-), 3017, 2363, 1680(C=O), 1586, 1524(Ar), 1420, 1308, 1206, 1101, 986, 804, 700; MS (ESI) m/z (%): 471.2 $[M+H]^+$, 493.2 $[M+Na]^+$.

2. 7 X-ray data collection and structure refinement

The white powder of compounds **5d** and **5e** was dissolved in ethanol/ethyl acetate/tetrahydrofuran = 5:2:3 (V/V/V) and 5:3:1 (V/V/V) mixed solvents, respectively. After slowly evaporating the solvents for several days, some single crystals suitable for X-ray analysis were obtained. The X-ray crystallography data for two crystals were collected on a Bruker APEX-II CCD automatic diffractometer with graphite-monochromatized Mo*Ka* radiation (λ = 0.71073 Å) using the φ and ω-scan mode at 296(2) K. The structure was solved by direct methods and refined with the SHELX crystallographic software package[13] and expanded by Fourier technique. The non-hydrogen atoms were refined anisotropically. The hydrogen atoms bound to carbon were determined with theoretical calculations and those attached to nitrogen and oxygen were determined with successive difference Fourier syntheses. Empirical absorption correction was applied. The structure was solved by direct methods

using SADABS[14]. The hydrogen atoms were placed at the calculated positions and refined as riding atoms with isotropic displacement parameters[15]. Crystallographic data and experimental details of structural analyses for **5d** and **5e** are summarized in Table 1. The hydrogen bonds of the title compound are listed in Table 2, and geometric parameters for it can be found in Table 3.

Table 1. Crystal Data of Compounds 5d and 5e

Compound	**5d**	**5e**
CCDC	2088950	2088951
Empirical formula	$C_{25}H_{20}ClFN_6O_2$	$C_{25}H_{19}ClF_2N_6O_2$
Formula weight	490.91	508.91
Crystal size (mm ^{3})	0.23 × 0.20 × 0.16	0.28 × 0.25 × 0.22
Crystal system	Monoclinic	Monoclinic
Space group	$P2_1/c$	$P2_1/c$
a (Å)	11.0500(10)	10.9998(18)
b (Å)	18.3045(17)	18.517(3)
c (Å)	13.5646(9)	13.6355(16)
α (°)	90	90
β (°)	122.806(5)	123.315(9)
γ (°)	90	90
Volume (Å^3)	2306.1(4)	2320.9(6)
Z	4	4
D_c (g·cm^{-3})	1.411	1.456
Index ranges	$-9 \leqslant h \leqslant 13$	$-12 \leqslant h \leqslant 13$
	$-21 \leqslant k \leqslant 21$	$-22 \leqslant k \leqslant 14$
	$-16 \leqslant l \leqslant 14$	$-16 \leqslant l \leqslant 15$
Absorption coefficient (μ)	0.210	0.218
F(000)	1012	1048
Theta range for data collection (°)	2.104 to 24.998	2.099 to 24.998
Reflections collected	11625	11670
Independent reflections	4051	4072
R_{int}	0.0273	0.0437
Goodness-of-fit on F^2	1.060	1.054
R, wR($I > 2\sigma(I)$)	R = 0.0606, wR = 0.2068	R = 0.0495, wR = 0.1139
R, wR(all data)	R = 0.0866, wR = 0.2263	R = 0.0943, wR = 0.1282

$R = \sum(||F_o|-|F_c||)/\sum|F_o|$, $wR = [\sum w(F_o^2-F_c^2)^2/\sum w(F_o^2)^2]^{1/2}$

Table 2. Hydrogen Bond Lengths (Å) and Bond Angles (°) of 5d and 5e

	D–H⋯A	d(D–H)	d(H⋯A)	d(D⋯A)	∠DHA
5d	N(1)–H(1)⋯N(5)	0.86	2.26	3.084(4)	160
	N(4)–H(4)⋯O(2)$^{\#1}$	0.86	2.06	2.871(4)	157
5e	N(1)–H(1)⋯N(5)$^{\#1}$	0.86	2.24	3.051(3)	159
	N(4)–H(4)⋯O(2)$^{\#2}$	0.86	2.06	2.874(2)	157

Symmetry codes: **5d**: #1: –*x*, *y*+1/2, –*z*+1/2; **5e**: #1: –*x*, –*y*, –*z*; #2: *x*, –*y*–1/2, *z*–1/2

Table 3. Geometric Parameters of 5d and 5e

Bond	Dist. for **5d**	Dist. for **5e**	Angle	**5d** (°)	**5e** (°)
C(1)–N(1)	1.397(4)	1.409(3)	C(6)–C(1)–N(1)	124.3(3)	122.9(3)
C(1)–C(2)	1.403(5)	1.387(4)	C(6)–C(1)–C(2)	118.6(3)	119.2(3)
C(3)–Cl(1)	1.745(4)	1.728(3)	N(2)–C(7)–N(3)	127.8(3)	127.5(2)
C(7)–N(2)	1.334(4)	1.341(3)	N(3)–C(7)–N(1)	114.5(3)	114.8(2)
C(7)–N(1)	1.381(4)	1.364(3)	C(8)–C(9)–C(10)	116.6(3)	116.2(3)
C(8)–C(9)	1.365(5)	1.358(4)	C(12)–C(11)–N(4)	119.8(3)	121.1(2)
C(10)–N(4)	1.357(4)	1.361(3)	C(18)–C(17)–C(21)	120.4(3)	120.1(3)

To be continued

C(11)–C(12)	1.388(5)	1.396(4)	N(5)–C(19)–N(6)	114.7(3)	114.5(2)
C(11)–N(4)	1.401(4)	1.405(3)	C(22)–C(23)–C(24)	117.5(3)	115.9(3)
C(14)–O(1)	1.382(4)	1.398(3)	C(24)–C(23)–C(25)	58.5(3)	58.6(2)
C(17)–C(18)	1.377(4)	1.377(4)	C(7)–N(1)–C(1)	127.6(3)	127.6(2)
C(17)–O(1)	1.379(4)	1.379(3)	C(7)–N(2)–C(10)	116.0(3)	115.9(2)
C(19)–N(5)	1.333(4)	1.338(3)	C(7)–N(3)–C(8)	113.8(3)	113.9(2)
C(19)–N(6)	1.399(4)	1.398(3)	C(22)–N(6)–C(19)	126.2(3)	126.2(2)
C(22)–O(2)	1.226(4)	1.230(3)	C(17)–O(1)–C(14)	117.7(2)	116.8(2)
C(22)–N(6)	1.362(4)	1.358(3)	N(1)–C(1)–C(2)–C(3)	–177.3(3)	175.3(2)
C(22)–C(23)	1.471(5)	1.464(4)	O(1)–C(14)–C(15)–C(16)	178.5(3)	178.3(2
C(23)–C(24)	1.507(5)	1.509(4)	N(2)–C(7)–N(1)–C(1)	–7.6(5)	6.1(4)
C(24)–C(25)	1.477(6)	1.469(4)	N(6)–C(22)–C(23)–C(25)	–133.3(3)	–163.5(2)

2. 8 *In vitro* anticancer activity test of the target compounds

The antiproliferative activities of compounds **5a~5f** were evaluated against human gastric cancer cell lines MKN-45, human colon cancer cell lines HT-29, human lung adenocarcinoma cell lines A549, human chronic myeloid leukemia cell lines K562 and human gastrointestinal stromal tumor cell lines GIST882 using the standard MTT assay *in vitro*, with Foretinib as the positive control. The cancer cell lines were cultured in minimum essential medium (MEM) supplement with 10% fetal bovine serum (FBS). Approximate 4×10^3 cells, suspended in MEM medium, were plated onto each well of a 96-well plate and incubated in 5% CO_2 at 37 °C for 24 h. The tested compounds at the indicated final concentrations were added to the culture medium and the cell cultures were continued for 72 h. Fresh MTT was added to each well at a terminal concentration of 5 μg/mL, and incubated with cells at 37 °C for 4 h. The formazan crystals were dissolved in 100 mL DMSO each well, and the absorbency at 492 nm (for absorbance of MTT formazan) and 630 nm (for the reference wavelength) was measured with an ELISA reader. All compounds were tested three times in each cell line. The results expressed as IC_{50} (inhibitory concentration 50%) were the averages of three determinations and calculated by using the Bacus Laboratories Incorporated Slide Scanner (Bliss) software.

3 RESULTS AND DISCUSSION

3. 1 Synthesis

The syntheses of target compounds **5a~5f** were outlined in Scheme 1. Commercially available 4-chloropyridin-2-amine was condensed with cyclopropanecarbonyl chloride in the presence of Et_3N to provide **1**, which underwent a nucleophilic substitution with 2-fluoro-4-nitrophenol to give the desired intermediate **2**. Reduction of the nitro group of **2** with iron powder and acetic acid in ethyl acetate/water (10:1 v/v) provided aniline compound **3**. **3** reacted with 2,4-dichloropyrimidine in refluxing *i*-PrOH to provide key intermediate **4** under the catalysis of DIPEA. **4** reacted with different substituted anilines in the presence of *p*-toluenesulfonic acid in refluxing *i*-PrOH to yield the target compounds **5a-5f**, and the their structures were confirmed by ^{1}H NMR, IR and ESI-MS.

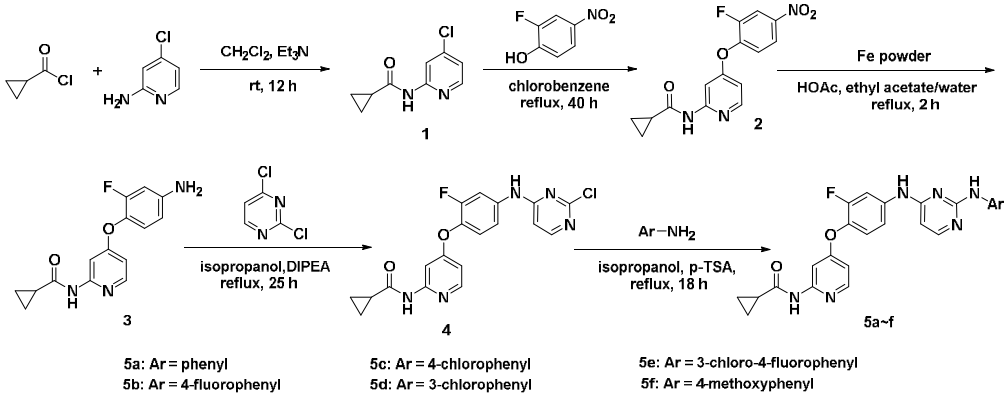

Scheme 1. Synthetic route and structure of target compounds

3. 2 Crystal structures

The structures of compounds **5d** and **5e** were further confirmed by single-crystal X-ray diffraction analysis. The molecular structures of compounds **5d** and **5e** with atom-numbering are shown in Fig. 2. Both crystal structures of **5d** and **5e** crystallize in monoclinic space group $P2_1/c$. Their crystal structures show that the two molecules have a 2,4-diarylaminopyrimidine skeleton, in which all bond lengths and bond angles fall in normal ranges. Both of the crystal structures consist of five rings: a three-membered cyclopropane (A), a pyrimidine ring (B), a pyridine ring (C) and two benzene rings (D, E). For compound **5d**, the molecule is not coplanar because the dihedral angles between rings A, B and C are 75.44° (A/C), 78.30° (A/B), 61.80° (A/D) and 33.91° (A/E), indicating rings B and C are almost perpendicular to ring A. For compound **5e**, the molecule is also not coplanar because the dihedral angles between rings A, B, C, D and E are 75.12° (A/C), 77.42° (A/B), 61.87° (A/D) and 47.67° (A/D), so similar perpendicular conformation is also found. For compounds **5d** and **5e**, the bond lengths of C(22)–O(2) are 1.226(4) and 1.230(3) Å belonging to the typical C=O double bond[16]. Meanwhile, hydrogen bonding interactions play a significant role in the crystal packing of **5d** and **5e** (Table 2). A mass of intermolecular hydrogen bonds N(4)–H(4A)⋯O(2), N(3)–H(6A)⋯N(6) and N(6)–H(6)⋯N(3) found in the two compounds play a major role in stabilizing the molecule. And the molecular structures of compounds **5d** and **5e** are shown in Fig. 3, depicting the molecular packing and hydrogen bonds in a unit cell. Within the molecule, the bond lengths and bond angles present no unusual features.

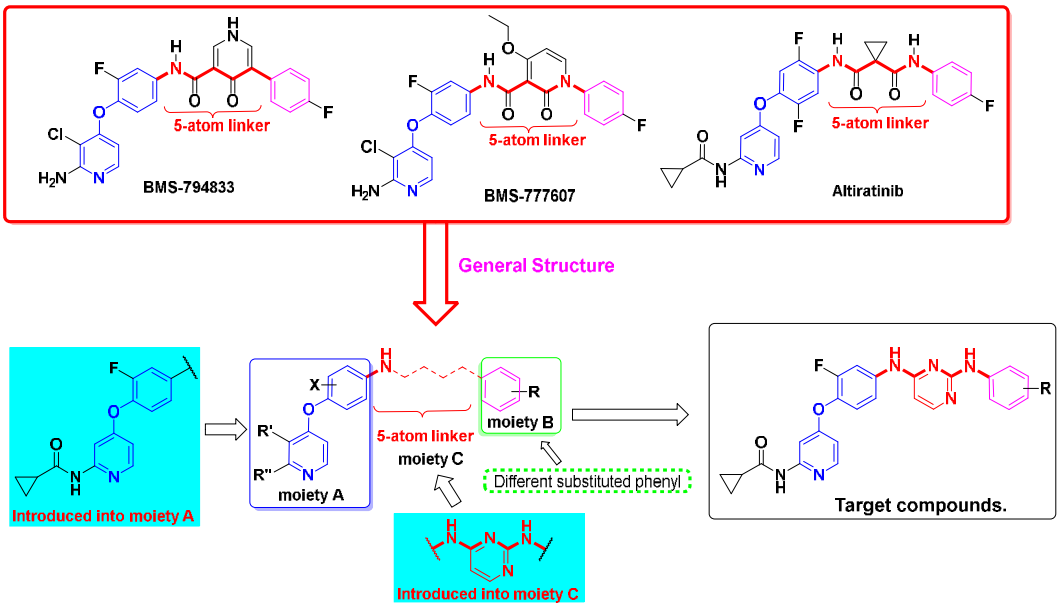

Fig. 1. The representative 4-phenoxypyridine type II c-Met kinase inhibitors and design strategy of the target compounds

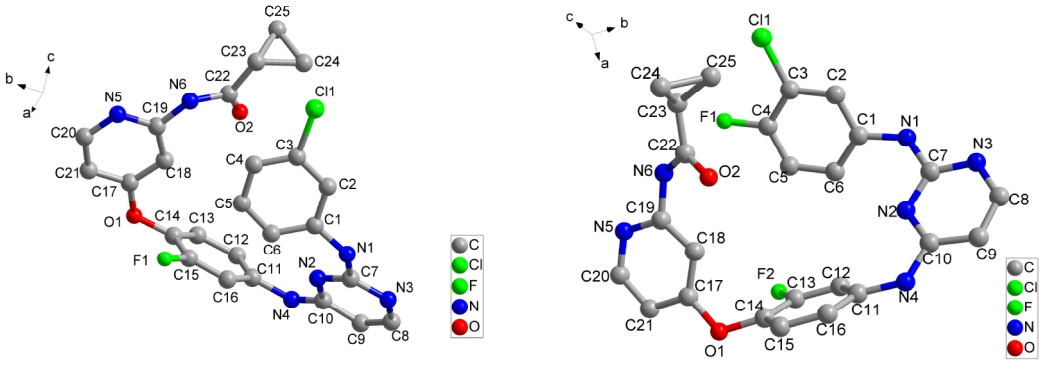

5d **5e**

Fig. 2. Molecular structure of compound 5d and 5e in a single crystal at 296 K

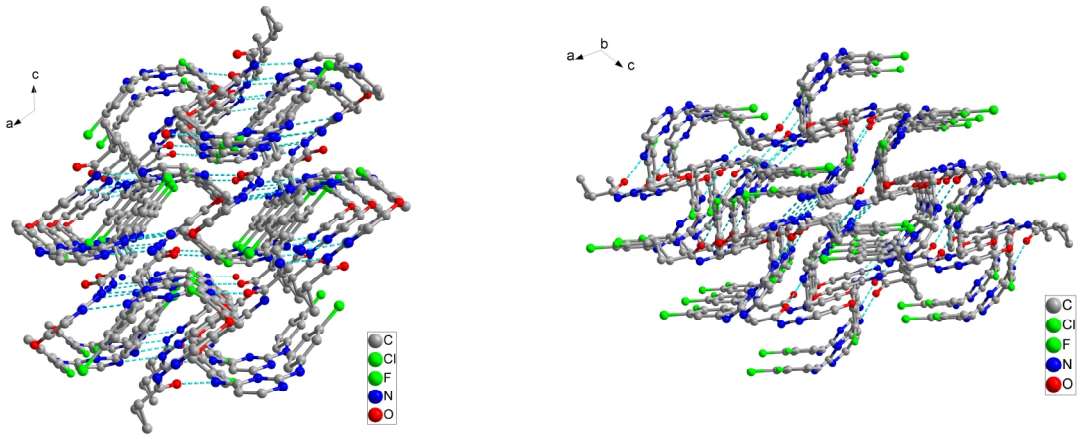

5d **5e**

Fig. 3. Crystal packing diagrams of compounds 5d and 5e

3. 3 Biological activity analysis

The IC_{50} values of **5a~5f** and Foretinib against MKN-45, HT-29, A549, K562 and GIST882 cancer cells are presented in Table 4, in which all the tested compounds show excellent antiproliferative activities against different cancer cells with IC_{50} values ranging from 0.38 to 6.29 μM, indicating that newly synthesized 4-phenoxypyridine derivatives maintained antitumor activities. Notably, compounds **5a** (R_1 = H), **5c** (R_1 = 4-Cl) and **5e** (R_1 = 3-Cl-4-F) exhibited remarkable antiproliferative activities against GIST882, K562 and A549 cell lines with IC_{50} values of 0.68 μM (foretinib: 0.75 μM), 0.38 μM (foretinib: 0.39 μM) and 0.60 μM (foretinib: 0.94 μM), respectively, which were all better than the positive control foretinib.

Table 4. Antiproliferative Activities of Target Compounds against Some Cancer Cells *in vitro*

Compd.	R_1	IC_{50} (μM)				
		MKN-45	HT-29	A549	K562	GIST882
5a	H	2.38	3.51	2.34	0.95	**0.68**
5b	4-F	1.26	2.09	2.25	0.61	1.92
5c	4-Cl	0.62	1.05	1.50	**0.38**	1.54
5d	3-Cl	1.36	2.36	2.23	1.01	2.85
5e	3-Cl-4-F	0.75	2.92	**0.60**	0.65	2.44
5f	4-CH_3	3.34	6.29	3.62	1.98	2.39
Foretinib	---	0.032	0.86	0.94	0.39	0.75

3. 4 Physicochemical and ADME parameters

Furthermore, some physicochemical and ADME properties of the synthesized compounds and positive controls were predicted using the SwissADME (a free web tool to evaluate pharmacokinetics, drug likeness and medicinal chemistry friendliness of small molecules) for their adaptability with Lipinski's rule of five[17-19]. Compounds obeying at least three of the four criteria are considered to adhere to Lipinski Rule.

As demonstrated in Table 5, the most active compounds show variable permeability based on gastrointestinal absorption (GI), according to the BOILED-Egg predictive model (Brain Or IntestinaL EstimateD permeation method). All predicted compounds showed high gastrointestinal absorption. With respect to oral bioavailability, it is expected 0.55 of probability of oral bioavailability score >10% in the rat for all compounds, the same as the control drug foretinib (0.55). Compound **5a~5f** exhibited potent *in vitro* antitumor activity, low toxicity and reasonable physicochemical properties, because suitable flexible and size in the bioavailability radar map (Fig. 4). All these data suggests that compound **5a~5f** could be considered as a candidate for further research.

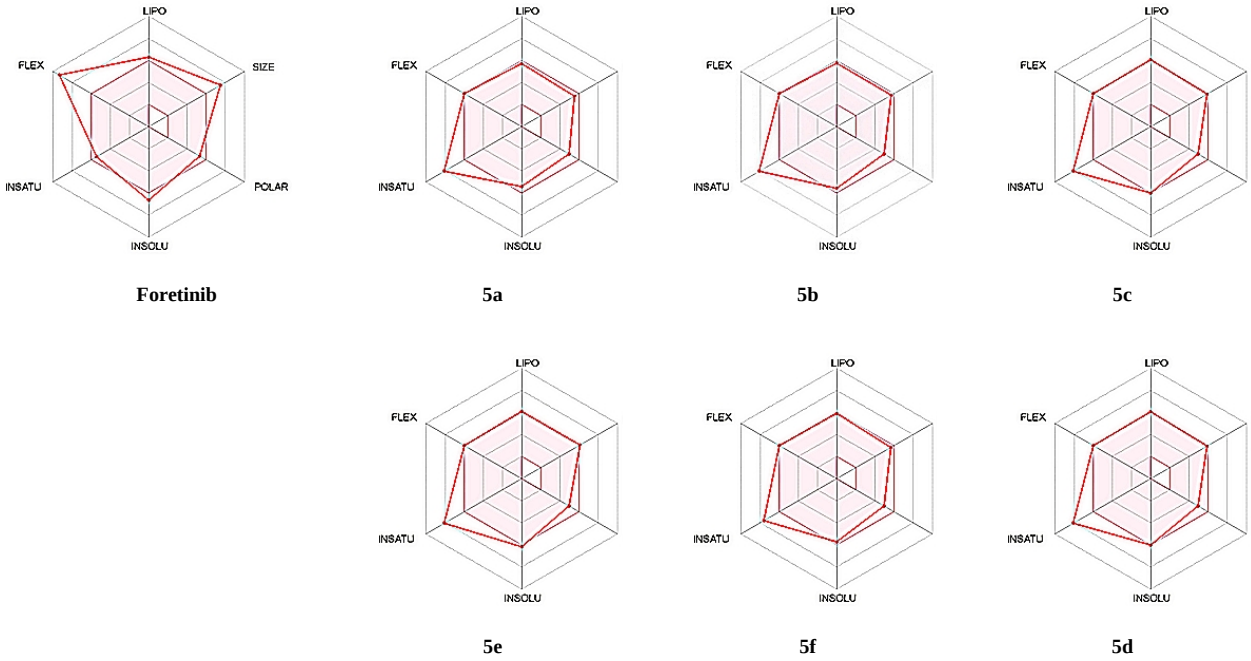

Fig. 4. The bioavailability radar enables a first glance at the drug-likeness of target compounds and Foretinib. The pink area represents the optimal range for each properties (lipophilicity: XLOGP3 between –0.7 and +5.0, size: MW between 150 and 500 g/mol, polarity: TPSA between 20 and 130 Å^2, solubility: logS not higher than 6, saturation: fraction of carbons in the *sp*^{3} hybridization not less than 0.25, and flexibility: no more than 9 rotatable bonds.

Table 5. Physicochemical Properties and ADME Properties of Target Compounds

Compd.	MW (g/mol) <500	H-bond acceptors <10	H-bond donors <5	Log P o/w <5	Violation Lipinski Rule of 5	[a]PSA (Å^2) ⩽140	Rotatable bonds <10	[b]BBB	[c]GI	[d]BS
5a	456.47	6	3	3.94	0	101.06	9	NO	Low	0.55
5b	474.46	7	3	4.13	0	101.06	9	NO	Low	0.55
5c	490.92	6	3	4.46	0	101.06	9	NO	Low	0.55
5d	490.92	6	3	4.41	0	101.06	9	NO	Low	0.55
5e	508.91	7	3	4.66	1	101.06	9	NO	Low	0.55
5f	470.50	6	3	4.12	0	101.06	9	NO	Low	0.55
Foretinib	632.65	10	2	4.80	1	111.25	14	NO	Low	0.55

[a]PSA – polar surface area. [b]BBB – blood-brain barrier. [c]GI – gastrointestinal absorption. [d]BS – bioavailability score.

Electronic supplementary information

Supplementary data associated with this article have been deposited in the ESI.

REFERENCES

(1) Lu, J. F.; Jin, L. X.; Ge, H. G.; Ji, X. H.; Guo, X. H.; Tian, G. H.; Song, J.; Jiang, M. Synthesis, crystal, computational study and biological activity of N-(1-(2,4-dichlorophenyl)-1H-pyrazolo[3,4-d]pyrimidin-4-y l)-4-(N,N-dipropylsulfamoyl) benzamide. *Chin. J. Struct. Chem.* **2017**, 36, 1810–1816.

(2) Chung, B. P. M.; Leung, D.; Leung, S. M.; Loke, A.Y. Beyond death and dying: how Chinese spouses navigate the final days with their loved ones suffering from terminal cancer. *Support. Care Cancer* **2018**, 26, 261–267.

(3) Tang, Q. D.; Zhao, Y. F.; Du, X. M.; Chong, L.; Gong, P.; Guo, C. Design, synthesis, and structure-activity relationships of novel 6,7-disubstituted-4-phenoxyquinoline derivatives as potential antitumor agents. *Eur. J. Med. Chem.* **2013**, 69, 77–89.

(4) Cai, Z. W.; Borzilleri, R. M. 4-pyridinone compounds and their use for cancer, WO2009094417, **2009**-07-30.

(5) Smith, B. D.; Kaufman, M. D.; Leary, C. B.; Turner, B. A.; Wise, S. C.; Ahn, Y. M.; Booth, R. J.; Caldwell, T. M.; Ensinger, C. L.; Hood, M. M.;

Lu, W. P.; Patt, T. W.; Patt, W. C.; Rutkoski, T. J.; Samarakoon, T.; Telikepalli, H.; Vogeti, L.; Vogeti, S.; Yates, K. M.; Chun, L.; Stewart, L. J.; Clare, M.; Flynn, D. L. Altiratinib inhibits tumor growth, invasion, angiogenesis, and microenvironment-mediated drug resistance via balanced inhibition of MET, TIE2, and VEGFR2. *Mol. Cancer Ther*. **2015**, 14, 2023.

(6) Dai, Y.; Siemann, D. W. BMS-777607, a small-molecule met kinase inhibitor, suppresses hepatocyte growth factor-stimulated prostate cancer metastatic phenotype *in vitro*. *Mol. Cancer Ther*. **2010**, 9, 1554–1561.

(7) Wang, Z.; Shi, J. T.; Zhu, X. L.; Zhao, W. W.; Gong, Y. L.; Hao, X. C.; Hou, Y. L.; Liu, Y. J.; Ding, S.; Liu, J.; Chen, Y. Design, synthesis and biological evaluation of novel 4-phenoxypyridine based 3-oxo-3,4-dihydroquinoxaline-2-carboxamide derivatives as potential c-Met kinase inhibitors. *Bioorg Chem.* **2020**, 105, 104371.

(8) Cui, H.; Peng, X.; Liu, J.; Ma, C. H.; Ji, Y. C.; Zhang, W.; Geng, M. Y.; Li, Y. X. Design, synthesis and biological evaluation of c-Met kinase inhibitors bearing 2-oxo-1,2-dihydroquinoline scaffold. *Bioorg. Med. Chem. Lett.* **2016**, 26, 4483–4486.

(9) Ma, P. C.; Tretiakova, M. S.; Nallasura, V.; Jagadeeswaran, R.; Husain, A. N.; Salgia, R. Downstream signalling and specific inhibition of c-MET/HGF pathway in small cell lung cancer: implications for tumour invasion. *Br. J. Cancer*. **2007**, 97, 368–377.

(10) Tang, Q. D.; Wang, L.X.; Tu, Y. Y.; Zhu, W. F.; Luo, R.; Tu, Q. D.; Wang, P.; Wu, C. J.; Gong, P.; Zheng, P. W. Discovery of novel pyrrolo[2,3-b]pyridine derivatives bearing 1,2,3-triazole moiety as c-Met kinase inhibitors. *Bioorg. Med. Chem. Lett*. **2016**, 26, 1680–1684.

(11) Liu, J.; Gong, Y. L.; Shi, J. T.; Hao, X. C.; Wang, Y.; Zhou, Y. P.; Hou, Y. L.; Liu, Y. J.; Ding, S.; Chen, Y. Design, synthesis and biological evaluation of novel *N*-[4-(2-fluorophenoxy)pyridin-2-yl]cyclopropanecarboxamide derivatives as potential c-Met kinase inhibitors. *Eur. J. Med. Chem.* **2020**, 194, 112244.

(12) Qi, B.; Tao, H.; Wu, D.; Bai, J.; Shi, Y.; Gong, P. Synthesis and biological evaluation of 4-phenoxy-6,7-disubstituted quinolines possessing semicarbazone scaffolds as selective c-Met inhibitors. *Arch. Pharm. Chem. Life Sci*. **2013**, 346, 596–609.

(13) Sheldrick, G. M. SHELXT − Integrated space-group and crystal-structure determination. *Acta Crystallogr*. **2015**, A71, 3–8.

(14) Sheldrick, G. M. SADABS, Program for Empirical Absorption Correction for Area Detector Data (Univ. of Göttingen, Göttingen, Germany, **1996**).

(15) Sheldrick, G. M. Crystal structure refinement with SHELXL. *Acta Crystallogr.* **2015**, C71, 3–8.

(16) Liu, W. R.; Hua, X. W.; Zhou, S.; Yuan, F. Y.; Wang, G. Q.; Liu, Y.; Xing, X. R. Design, synthesis and biological activity of N-sulfonyl aromatic amide derivatives. *Chin. J. Struct. Chem.* **2021**, 40, 666–674.

(17) Lipinski, C. A.; Lombardo, F. B.; Dominy, W.; Feeney, P. J. Experimental and computationalapproaches to estimate solubility and permeability in drug discovery and development settings. *Adv. Drug Deliv. Rev*. **1997**, 23, 3–25.

(18) Veber, D. F.; Johnson, S. R.; Cheng, H. Y.; Smith, B. R.; Ward, K. W.; Kopple, K. D. Molecular properties that influence the oral bioavailability of drug candidates. *J. Med. Chem.* **2002**, 45, 2615–2623.

(19) de Santana, T. I.; Barbosa, M. D.; Gomes, P. A. T. M.; da Cruz, A. C. N.; da Silva, T. G.; Leite, A. C. L. Synthesis, anticancer activity and mechanism of action of new thiazole derivatives. *Eur. J. Med. Chem.* **2018**, 144, 874–886.